23rd ABCM International Congress of Mechanical Engineering
December 6-11, 2015, Rio de Janeiro, RJ, Brazil

AERODYNAMICS STABILITY DERIVATIVES IDENTIFICATION OF A SEA SKIMMING MISSILE

Fernando Antonio Almeida Coelho
Marinha do Brasil.
R. Primeiro de Março, 118. Ed. Barão de Ladário, 21º Andar. Centro. Rio de Janeiro - RJ
feraac@gmail.com

Elder Moreira Hemerly
Instituto Tecnológico de Aeronáutica.
Praça Mal. Eduardo, 50, Vila das Acácias, CEP 12228-900, São José dos Campos - SP
hemerly@ita.br

Abstract. *The missile aerodynamics parameters identification is a necessary step for designing a high performance missile control system. Hence, typically extensive testing in wind tunnels is required, that are not always readily available, in addition to the demand of time and financial resources. Two alternatives arise to overcome these difficulties: i) the so-called engineering methods, in which there are semi-empirics formulas that allow estimating the derivatives of aerodynamic stability with up to 20% errors, according to the literature; and ii) the methods of CFD (Computational Fluid Dynamics), that require specific knowledge and a good deal of intuition to ensure appropriate convergence of the estimates. Therefore, the uncertainties present in such alternatives require the use of a robust controller, which generally are conservative from the performance point of view. As an alternative to the model refinement, this work investigates the possibility of identifying the longitudinal dynamics of a sea skimming missile when maneuvers are restricted to its normal flight profile, which may not be exciting enough for identifying the parameters. Simulation results using Simulink and the X-Plane flight simulator allowed the model refinement and parameter identification with only a simple maneuver of decline in altitude. Open-loop and closed-loop configurations, as well as several combinations of input and output signals, were examined and efficient identification was achieved by using reference altitude as input, and the pitch angular velocity, angle of attack, altitude and speed as outputs.*

Keywords: *parametric identification, aerodynamics derivatives estimation, missile flight dynamics*

1. INTRODUCTION

One of the most important tasks in a missile development is the aerodynamics coefficients prediction, mainly because uncertainty in these parameters impact directly on the performance requirements (Briggs, 1992). Thus, extensive tests in wind tunnels are required, which are not always readily available and can impact on the budget or time schedule of the program. By this reason, during the early stages of the project, the autopilot designer must work with aerodynamic data predicted by semi-empirics or CFD (Computational Fluid Dynamics) methods. Unfortunately, these methods may have up to 20% intrinsic errors, according to some studies (Sooy & Shmidt, 2004; Rdluan,2014), requiring a later refinement of these predictions.

This work proposes the use of a robust controller to overcome these uncertainties, in the first approach. Later, the refinement of the aerodynamics is achieved by identifying the model, with real flight data extracted from the first flight tests. As the missile under study performs a sea skimming profile, its maneuvers are restricted, hence may not be exciting enough to estimate the parameters. Thus, this work investigates the possibility of identifying the longitudinal dynamics of a sea skimming missile under a normal profile maneuver.

A nonlinear model is employed, as presented in Section 2. The output error method is used to perform a gray box identification, in Section 3. In Section 4, the simulations of the dynamics performed with Simulink are presented, to investigate the estimation convergence with diferent configurations of inputs, and also in open and closed-loop operation. In Section 5, results obtained from simulated flight data extracted from the X-Plane flight simulator are presented. On this simulator, aerodynamic forces are calculated in real time by the blade element theory, hence aerodynamics stability derivatives are not used directly. This makes the experiment more realistic (Laminar Research, 2015). Section 6 presents the main conclusions.

2. MATHEMATICAL MODEL

In this work the missile is modeled as a rigid body according to the dynamic Eqs. (1) to (6) (Coelho, 2007):

$$\dot{v}_x = \frac{F_x}{m} - v_z\omega_y \quad (1)$$

$$\dot{v}_z = \frac{F_z}{m} + v_x\omega_y \quad (2)$$

$$\dot{\omega}_y = \frac{M_y}{I_y} \quad (3)$$

$$\dot{\phi}_y = \omega_y \quad (4)$$

$$\dot{h} = v_x \sin(\phi_y) - v_z \cos(\phi_y) \quad (5)$$

$$\dot{m} = d_m \quad (6)$$

where v_x and v_z are the velocities along the longitudinal and transversal (yawing) axis, respectively; ω_y is the pitch angular rate; ϕ_y is the pitch angle; h is the altitude or the height from the sea mean level; m is the mass; I_y is the moment of inertia about the pitch axis; d_m is a constant rate of loss of mass; M_y is the pitching moment; F_x and F_z are the forces along the longitudinal and transversal axis, respectively.

The forces are calculated by

$$F_x = -D\cos(\alpha) - mg\ \sin(\phi_y) + P \quad (7)$$

$$F_z = -L\cos(\alpha) + mg\cos(\phi_y) \quad (8)$$

where α is the angle of attack given by $\alpha = \mathrm{atan}(v_z/v_x)$; g is the gravity acceleration; P is the propulsion thrust; D is the aerodynamic drag; L is the aerodynamic lift; and these aerodynamics forces and moment, M, are calculated by

$$L = qS_{ref}\left(C_{L\alpha}\alpha + C_{L\delta_e}\delta_e\right) \quad (9)$$

$$D = qS_{ref}\left(C_{D_0} + C_L^2/\pi A_R\epsilon\right) \quad (10)$$

$$M = qS_{ref}\left(C_{M\alpha}\alpha + C_{M\delta_e}\delta_e\right) \quad (11)$$

where q is the dynamic pressure given by $q = \rho V^2/2$; with ρ being the air density, and V the missile velocity; S_{ref} is the reference area; $C_{L\alpha}$ is the aerodynamic lift derivative with respect to the angle of attack; $C_{L\delta_e}$ is the aerodynamic lift derivative with respect to the elevator angle, δ_e; C_{D_0} is the minimum aerodynamic drag coefficient; C_L is the aerodynamic lift coefficient given by $C_L = L/q/S_{ref}$; $C_{M\alpha}$ is the aerodynamic pitch moment derivative with respect to the angle of attack; $C_{M\delta_e}$ is the aerodynamic pitch moment derivative with respect to the elevator angle; A_R is the aspect ratio given by $A_R = b^2/S_{ref}$, with b being the wing span; and ϵ is the Oswald efficiency factor.

As the missile propulsion consumes the solid propeller during flight, the mass of the missile is variable as indicated by Eq. (6). In the same way, the moment of inertia varies according to

$$I_y = mk^2 \quad (12)$$

where k is the radius of gyration to be estimated during the identification process.

The actuator dynamics considered is only a delay, and is regarded as previously identified.

The vector of components to be estimated, $\boldsymbol{\Theta}$, include the physical parameters, the six initial states of the plant, v_{x0}, v_{z0}, ω_{y0}, ϕ_{y0}, h_0 and m_0, and two initial states of a PID digital controller, x_{I_0}, x_{D_0}, as presented in Eq. (13).

$$\boldsymbol{\Theta} = [P \quad k \quad d_m \quad C_{L\alpha} \quad C_{L\delta_e} \quad C_{D_0} \quad \epsilon \quad C_{M\alpha} \quad C_{M\delta_e} \quad x_{I_0} \quad x_{d_0} \quad v_{x0} \quad v_{z0} \quad \omega_{y0} \quad \phi_{y0} \quad h_0 \quad m_0]^T \quad (13)$$

Especial attention must be done when performing nonlinear identification of parameter that are summed or divided one to the other. This is the case of the propulsion thrust, P, that is summed to drag force. This is also the case of the parameters related with the mass, m_0 and d_m, because the mass divides forces in Eq. (1) and (2). Thankfully these parameters can be predicted accurately by essay in static conditions during development of the propulsion motor. Even though, they were included in Eq. (13) to analyze their sensitivity to this issue. Besides, as X-Plane calculates the radius of gyration, k, by itself, this parameter was included in Eq. (13).

3. OUTPUT ERROR METHOD

The output error method, illustrated in Fig. 1, is well explained in Jategaonkar (2006). A summary is presented here. It is one of the most widely applied time-domain method to estimate aircraft parameters. In this method, the model parameters are adjusted to minimize the error between the system measured outputs, $\boldsymbol{z}(t)$, and the model prediction (responses estimated by the model), $\boldsymbol{y}(t)$, where t is sampled time. A nonlinear optimization method must be applied to minimize the prediction error. The weighted least squares method is the simplest one, but requires the weights to be previously defined. This does not occur with the maximum-likelihood estimator, which is in general the preferred method.

For applying the maximum-likelihood method, some assumptions are necessary. Two of these assumptions are particularly important for this research. The first one is that the input sequence $[\boldsymbol{u}(t),\ t = 1, 2, \ldots, N]$ must be exogenous, that is, no output feedback is present on this signal. As the missile in this work is unstable, some feedback stabilization must be performed a priori. Therefore, special treatment for the identification is required. One possible solution is the addition of a command directly to the control surfaces, via a bypass, when performing the open loop identification. However, as will be seen on Section 4, this problem was not verified in simulation, and no intervention in the input signal was necessary. The second assumption is that the control inputs $\boldsymbol{u}(t)$ must be adequately changed to excite the several dynamical modes. As the missile in sea skimming has the flight profile limited in altitude, simulations were carried out to verify if this excitation condition is satisfied, and special maneuvers are considered if not.

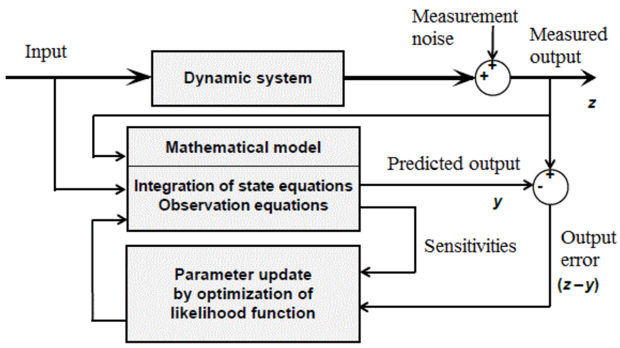

Figure 1. Block diagram for the output error method (adapted from: Jategaonkar (2006))

The maximum-likelihood estimation leads to the minimization of the following cost function for N data points, and n_y observation variables

$$J(\boldsymbol{\Theta}, \boldsymbol{R}) = \frac{1}{2}\sum_{t=1}^{N}[\boldsymbol{z}(t) - \boldsymbol{y}(t)]^T \boldsymbol{R}^{-1}[\boldsymbol{z}(t) - \boldsymbol{y}(t)] + \frac{N}{2}\ln\left[(\det(\boldsymbol{R})\right] + \frac{Nn_y}{2}\ln(2\pi) \tag{14}$$

where $\boldsymbol{R}$ is the measurement noise covariance matrix.

If $\boldsymbol{R}$ is known, the last two terms in Eq. (14) are constants, and the cost function can be modified to

$$J(\boldsymbol{\Theta}, \boldsymbol{R}) = \frac{1}{2}\sum_{t=1}^{N}[\boldsymbol{z}(t) - \boldsymbol{y}(t)]^T \boldsymbol{R}^{-1}[\boldsymbol{z}(t) - \boldsymbol{y}(t)] \tag{15}$$

However, in the most cases the covariance is unknown, and one can estimate it at each iteration of the optimization procedure by using the sample average

$$\boldsymbol{R} = \frac{1}{N}\sum_{t=1}^{N}[\boldsymbol{z}(t) - \boldsymbol{y}(t)][\boldsymbol{z}(t) - \boldsymbol{y}(t)]^T \tag{16}$$

By replacing Eq. (16) in (14), the cost function can be reduced to

$$J(\boldsymbol{\Theta}, \boldsymbol{R}) = \ln\left[(\det(\boldsymbol{R})\right] \tag{17}$$

Defined the cost function, an optimization algorithm must be employed. In this paper, the Levenberg-Marquardt method is used. It is based on the well known Gauss-Newton method combined with the steepest-descent technique.

Figure 2 shows the block diagram of the system augmented by the controller. To perform closed-loop identification, the command of altitude, h_{ref}, is used as the input, u. Otherwise, for open-loop identification, the elevator angle, δ_e, is considered as input. In this case a bypass permits the addition of direct elevator angle command, in order to deal with the presence of feedback, as discussed previously in this section. Nevertheless, we verified in simulations that the use of this bypass was not necessary.

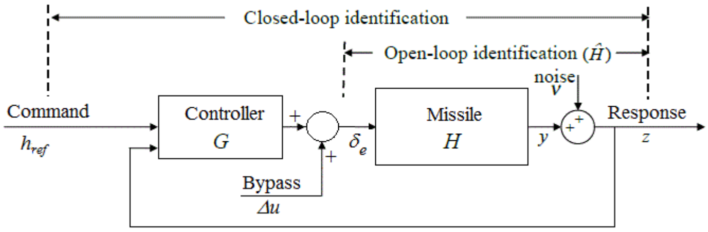

Figure 2. Block diagram of the system augmented by the controller (adapted from: Jategaonkar (2006))

4. SIMULATIONS

The mathematical model presented in Section 2 was implemented in Simulink to generate synthetic data for the identification algorithm. Typical parameters were used as listed in Tab. 1. Based on these parameters, a digital controller with sampler rate of $20Hz$ was designed in order to achieve stabilization and altitude regulation. The controller consists of a negative feedback of the pitch angle, ϕ_y, and angular velocity, ω_y, with gains $k_{\phi_y} = 0.014$, $k_{\omega_y} = 0.25$, and a PID altitude regulator with gains $k_P = 0.05$, $k_I = 0.03$ e $k_D = 0.05$. The integrator of the PID regulator also incorporates an anti-windup saturation with ± 0.35 in amplitude. Besides, it is introduced a saturation of $\pm 40°$ on the elevation command.

The missile has an initial mass of $855kg$ and is accelerated, during 3 seconds, from zero to at least $310m/s$, while consumes $100kg$ of propeller. After this phase the missile maintains its velocity practically constant by a sustain rocket motor with a rate of loss of mass $d_m = -1.28kg/s$ and thrust $P = 2{,}756$ Newtons.

Table 1. Parameters used to simulate the missile

Parameter	$P\ (N)$	$k\ (m)$	$d_m\ (kg/s)$	$C_{L\alpha}$	$C_{L\delta_e}$	C_{D_0}	ϵ	$C_{M\alpha}$	$C_{M\delta_e}$
Value	2,756	1.21	-1.28	6.65	-0.20	0.07	0.55	-2.37	0.60

Figure 3 shows the measurements during the missile launching and two height descend steps. Initially the missile altitude is commanded to 30 meters and, after the flight is trimmed, two descend maneuver are commanded, one to 15 meters, at $10s$, and the other to 8 meters, at $20s$. Only the first descend maneuver is used for identification, while the second one can be used for validation.

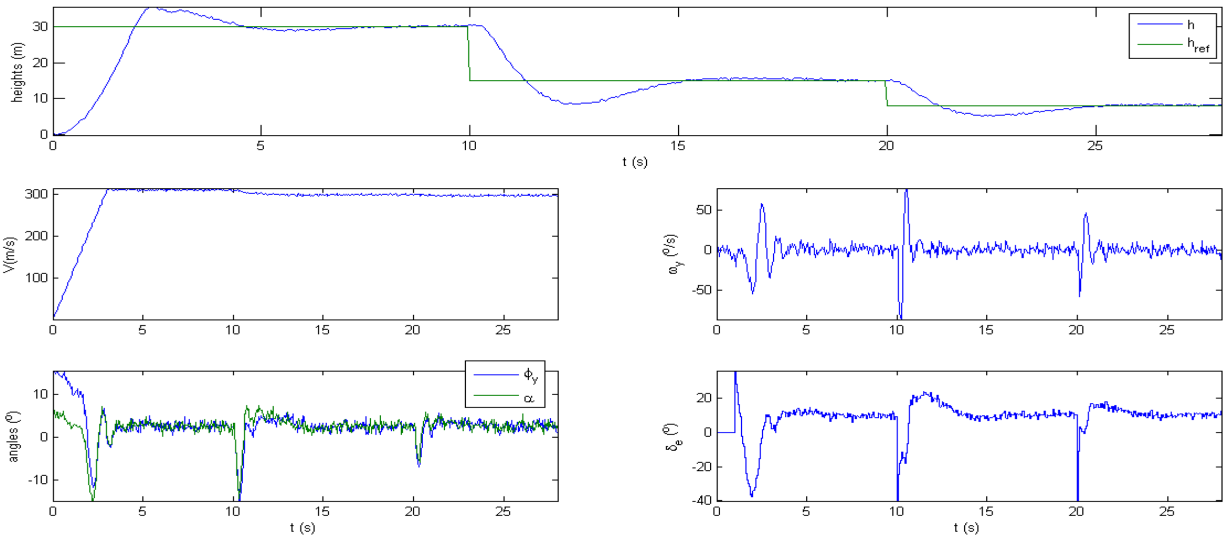

Figure 3. Measurements during the maneuver of descend in altitude

Five signals shown on Fig. 3 were considered as output, ω_y, ϕ_y, α, h, V, while h_{ref} and δ_e were used as input in closed loop or open loop identification, respectively. During simulation, white Gaussian noise with standard deviation of 0,1% of the maximum value was added to the velocity and altitude, and 1% to the others measures, what represent a signal to noise ratio of 40 and $60dB$, respectively. These measures with noise were feedback to the controller, with exception to the derivative of element of the PID controller, which received the noiseless altitude. This is to avoid noise amplification. In practice this signal would be filtered.

The typical uncertainty of engineering methods of aerodynamic derivatives prediction, $\pm 20\%$, was randomly added to the nominal parameters values and initial conditions to use as a first guess for the estimative. The Matlab function *fmincon()* was used to minimize the cost function of Eq. (17), constrained to these typical maximum errors.

4.1 Identification of Initial Mass and Propulsion Parameters

In order to verify the possibility of identifying the initial mass and propulsion parameters, we performed a first identification and the result is shown on Fig. 4 and Tab. 2. Figure 4 shows the main predicted outputs after open loop identification. The closed loop predictions are similar, so are omitted in this figure. Table 2 compares the nominal parameters and initial guess with estimated ones.

Analyzing the estimates in Tab. 2, one can see that the propulsion thrust, P, and the initial mass, m_0, remains almost the same as the initial guess. As commented earlier in Section 2, mass and propulsion parameters can influence the estimates of the aerodynamic coefficients, what explains the errors of the aerodynamics derivatives still near the maximum uncertainty ($\pm 20\%$). Thus, we started by considering the parameters P, d_m, and m_0 as previously estimated. In fact they can be reasonably estimated by static experiments during development of the propulsion.

Table 2. Estimates of the parameters in open and closed loop in comparison with the nominal values

Parameter	$P\ (N)$	$k\ (m)$	$m_0\ (kg)$	$d_m\ (kg/s)$	$C_{L\alpha}$	$C_{L\delta_e}$	C_{D_0}	ϵ	$C_{M\alpha}$	$C_{M\delta_e}$
Nominal values	2,756	1.21	747.0	-1.28	6.65	-0.20	0.070	0.55	-2.37	0.60
Initial guess	2,436	1.09	608.0	-1.04	7.91	-0.22	0.060	0.47	-2.56	0.57
Open loop estimates	2,436	1.37	608.2	-1.19	5.40	-0.16	0.065	0.45	-2.48	0.63
Closed loop estimates	2,436	1.43	608,1	-1.46	5.58	-0.21	0.065	0.46	-2.71	0.69
Open loop errors (%)	-12%	13%	-19%	7%	-19%	20%	-7%	-18%	-5%	5%
Closed loop errors (%)	-12%	18,2%	-19%	-14%	-16%	-5	-7%	-16%	-14%	15%

Table 3 shows the new estimates with the propulsion parameters fixed to nominal. In this case, most errors were reduced consistently. However, the estimate of $C_{L\delta_e}$ in closed loop identification remains pretty close to the maximum uncertainty. The no convergence of the parameter $C_{L\delta_e}$ can be explained by two facts: the absence of sufficient excitation of the input, h_{ref}, in high frequencies; and the fact that the lift force is mainly caused by the angle of attack. This parameter is even negligible in some missile modeling, as in How & Duan (2011).

From the good fitting between the measured and predicted outputs in Fig. 4, one can see that, even if the closed loop parameters estimates are near the uncertainty of $\pm 20\%$, the identification adjusts the parameters to have a better output prediction, thereby improving the model. This is helpful for redesigning the controller gains, making the identification useful in any case.

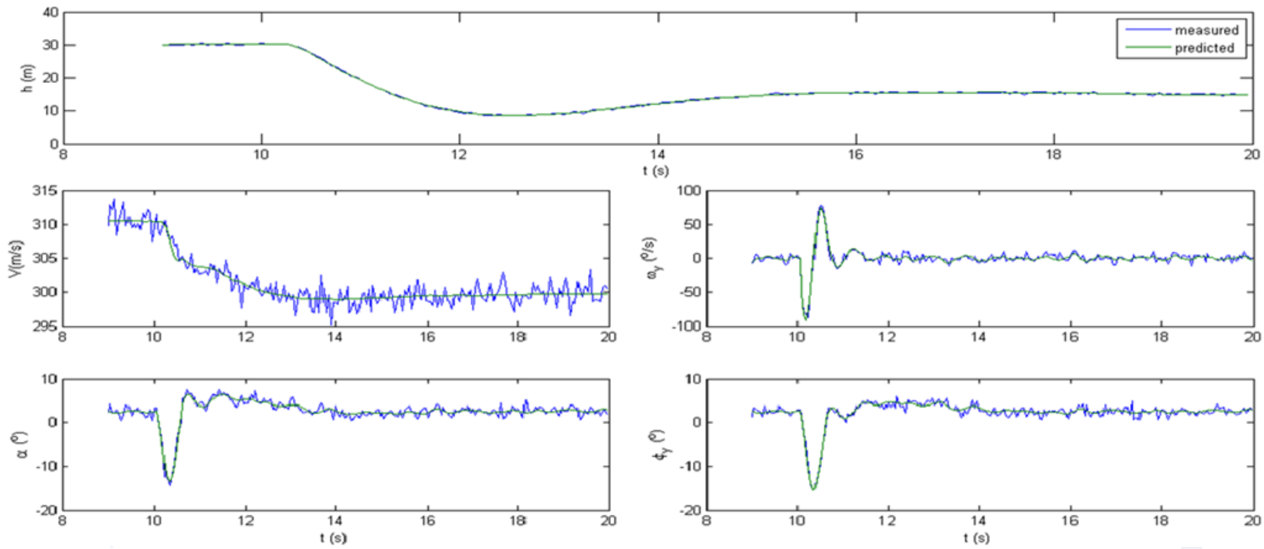

Figure 4. Predicted and measured outputs after identification in open loop

Table 3. Estimates with propulsion parameters and initial mass fixed to nominal value.

Parameter	$k\ (m)$	$C_{L\alpha}$	$C_{L\delta_e}$	C_{D_0}	ϵ	$C_{M\alpha}$	$C_{M\delta_e}$
Open loop estimates	1.16	6.62	-0.19	0.071	0.552	-2.198	0.556
Closed loop estimates	1.20	6.82	-0.24	0.071	0.559	-2.373	0.601
Open loop errors (%)	-4%	-0.5%	-5%	1.4%	0.4%	-7%	-7%
Closed loop errors (%)	-0.8%	2.6%	-20%	1.4%	1.6%	-0.1%	0.2%

4.2 Comparison Between Open and Closed Loop Identifications

Since the predictions for open and closed loop identification do not differ considerably, another analysis procedure is necessary. Figure 5 shows the autocorrelation of the outputs prediction errors. From this figure, one can see that the autocorrelation remains closer to the zero for open than for closed loop identification. In fact, the determinant of the error covariance matrix, Eq. (13), results $\det(\boldsymbol{R}) = 6.3 \times 10^{-17}$ for open loop, and $\det(\boldsymbol{R}) = 2{,}1 \times 10^{-16}$ for the closed loop, i.e., the outputs predictions errors have covariance greater for the closed than the open loop identification. This is curious because, in closed loop, the presence of measurements feedback could have degraded the identified model. Again, this can be explained by the fact that dynamics of higher frequencies are better estimated in open than in closed loop configuration.

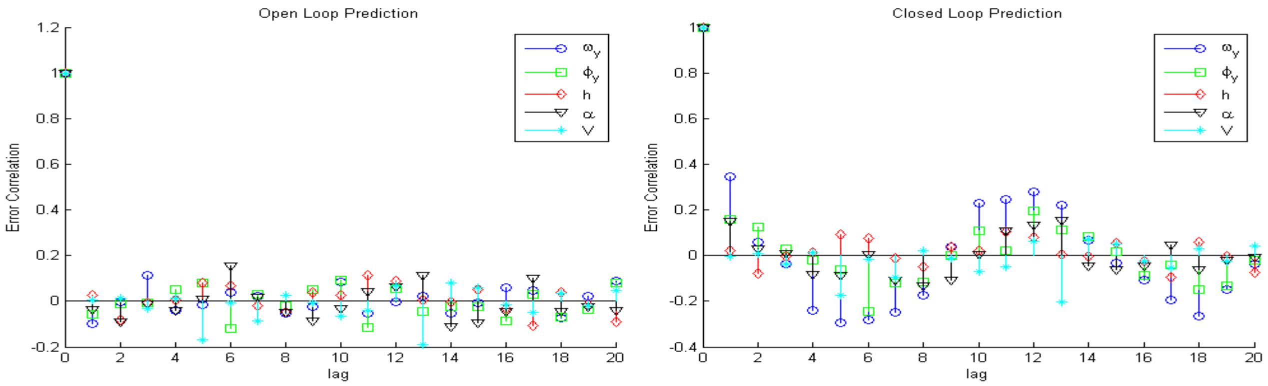

Figure 5. Autocorrelation of the outputs predictions errors for open and closed loop identification

4.3 Relevant Outputs for Identification

To analyze which measurements are relevant, we performed the identification without some of the five available outputs. Table 4 shows the rounded errors resulted from this procedure.

From first and third data rows of Tab. 4, it is possible to conclude that the exclusion of the angle of attack, α, affect directly the quality of the estimates of the parameters related with the pitch moment, $C_{M\alpha}$ and $C_{M\delta_e}$. On the other hand, exclusion of the pitch angle, θ_y, (2nd row) results in errors in the same order of magnitude shown in Tab. 3, indicating that this measurement is negligible.

When the velocity is not used (last four rows), mainly the parameters related to aerodynamic drag, C_{D_0} and ϵ, diverge, and others parameters also degrade, indicating that this output is important for the identification. This is due to the fact that the velocity affects the dynamic pressure, q, which is present in all the aerodynamic forces Eqs. (9) to (11).

Table 4. Parameters estimates percentage errors for different configuration of measurements

		Open loop identification errors (%)							Closed loop identification errors (%)						
Parameter		k	$C_{L\alpha}$	$C_{L\delta_e}$	C_{D_0}	ϵ	$C_{M\alpha}$	$C_{M\delta_e}$	k	$C_{L\alpha}$	$C_{L\delta_e}$	C_{D_0}	ϵ	$C_{M\alpha}$	$C_{M\delta_e}$
Measurements	ω_y, ϕ_y, h, V	3	0	0	1	1	-6	6	4	2	-17	1	1	-8	6
	ω_y, α, h, V	-1	-1	-5	1	0	-2	-3	2	2	20	1	2	5	5
	ω_y, h, V	4	0	-3	1	0	8	8	1	2	-18	1	1	-4	4
	$\omega_y, \phi_y, \alpha, h$	3	-1	-12	6	20	5	5	1	2	20	1	20	1	1
	ω_y, ϕ_y, h	9	-1	8	6	20	-20	19	8	2	-20	-5	20	-18	18
	ω_y, α, h	9	-2	-15	6	20	20	20	0	2	20	8	20	3	3
	ω_y, h	-2	-1	-9	5	20	-4	-4	16	-17	12	-3	20	-15	15

5. RESULTS WITH ARTIFICIAL FLIGHT DATA

In order to perform a more realistic experiment, we used the X-Plane Simulator to collect flight data for identification. The missile was designed using the X-Plane auxiliary program called Plane Maker. With the aid of this CAD (Computer-Aided Design) software, several sorts of airplanes can be modeled to be used by X-Plane, as can be seen in Laminar Research (2010). The simulator was linked to Simulink to implement the digital controller, as described in Ribeiro (2011).

As the noises in this test platform were considered too low, we added noises to the measures in the same level as in Section 4. A delay of one sampler period, $\tau = 0.05s$, between the Simulink and X-plane was previously identified and introduced to the missile model as a transport delay.

As cited by Dorfling & Rokhsaz (2014), blade element theory does not perform well with low aspect ratio airplanes. As X-Plane uses this method to calculate the aerodynamic forces, is expected that the aerodynamics derivatives estimated have more uncertainties than the simulations performed in Section 4. Thus we adopted 30% as constrains for the parameters estimates, instead of the 20% of Section 4. The initial estimates applied were the nominal ones. The pitch angle, θ_y, was not considered as output, since the analyses made in Section 3 considered it irrelevant for identification.

Table 5 shows the estimates in open and closed loop configuration, while Fig. 6 shows the predicted angle of attack, α, in comparison with the measured one. The determinant of the error covariance matrix, Eq. (13), resulted $\det(\boldsymbol{R}) = 1 \times 10^{-9}$ for open loop, and $\det(\boldsymbol{R}) = 2 \times 10^{-11}$ for the closed loop.

Table 5. Estimates with data extracted from X-Plane simulator.

Parameter	$k\ (m)$	$C_{L\alpha}$	$C_{L\delta_e}$	C_{D_0}	ϵ	$C_{M\alpha}$	$C_{M\delta_e}$
Open loop estimates	1.13	7.08	-0.26	0.05	0.53	-2.29	0.58
Closed loop estimates	1.22	6.02	-0.14	0.05	0.53	-2.53	0.71
Open loop errors (%)	-7%	7%	-30%	-29%	-3%	3%	-4%
Closed loop errors (%)	0.5%	-9%	30%	-29%	-4%	-7%	19%

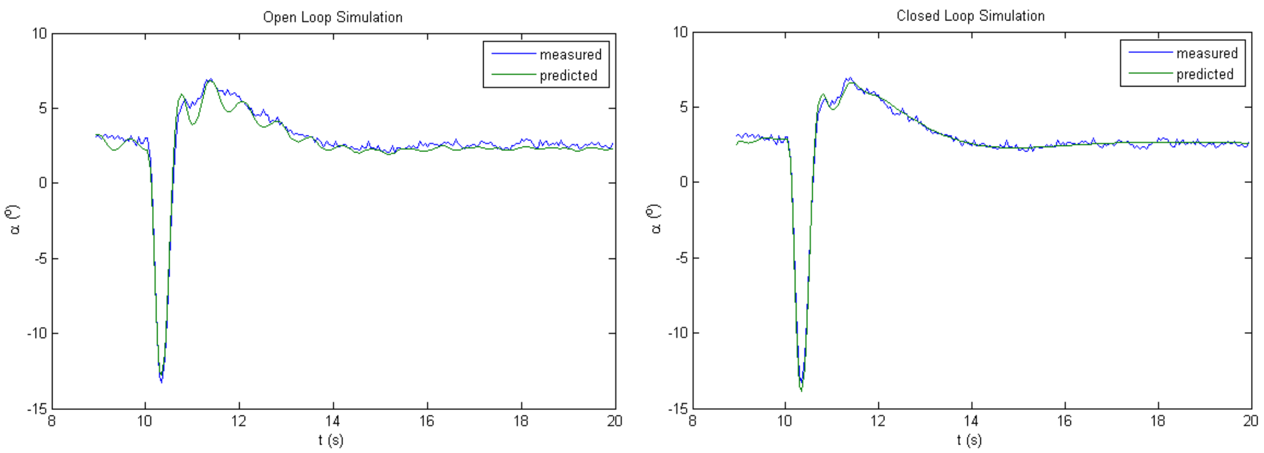

Figure 6. Predicted angle of attack, α, in open (left) and closed (right) loop configuration.

From these results, one can conclude that the closed loop configuration generate more accurate estimates, differently of what happened in simulation of Section 4. This is due to the fact that in Section 4 we used the same model to simulate the missile and to predict the outputs, while the dynamics calculated by X-Plane is different. This difference between the model and the real dynamics reflects mainly in the open loop estimates, because there is no feedback to compensate these errors. As an example, we tried a different model introducing an additional term in Eq. (11), proportional to the angular velocity, $C_{M\omega_y}\omega_y$. In this case, the determinant of the error covariance matrix, Eq. (13), reduced slightly to $\det(\boldsymbol{R}) = 1 \times 10^{-11}$.

It should be noted, from Tab. 5, that the estimates of $C_{L\delta_e}$ still diverges, even in closed loop configuration, for the reasons already explained in Section 4.

To validate the identification performed, the parameters estimated in closed loop were used to predict the outputs in a second descend maneuver as shown in Fig. 7. This figure shows a good fitting of the predictions to the outputs, with exception to the velocity. This divergence of the velocity can be explained by the fact that there is no speed control loop in the plant.

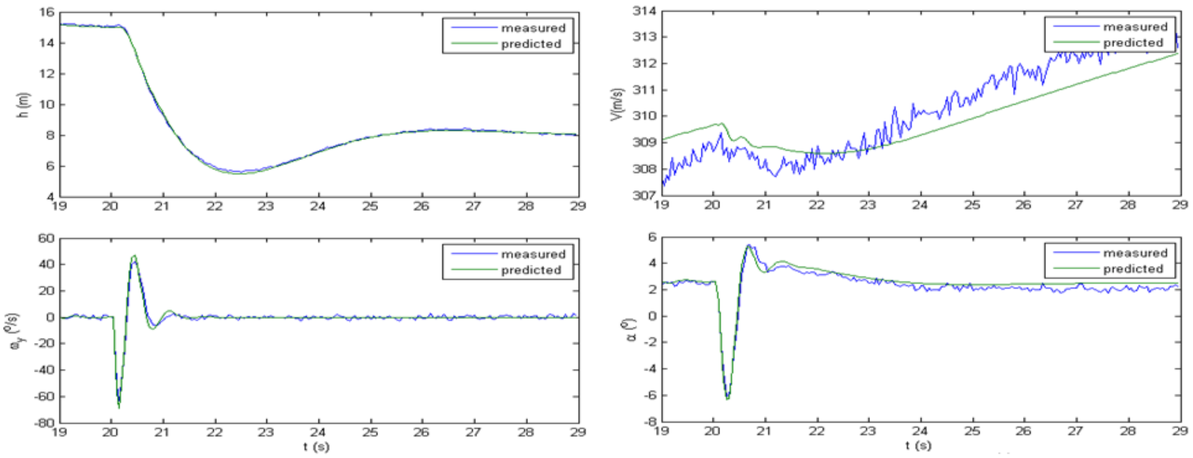

Figure 7. Maneuver for model validation

6. CONCLUSIONS

This work investigated the possibility of identifying the longitudinal dynamics of a sea skimming missile, when maneuvers are restricted to its normal flight profile, in both closed and open loop configuration. Simulations using Simulink and X-Plane flight simulator allowed the conclusion that the closed loop configuration is less sensitive to errors of modeling than the open loop one.

In some cases the parameters do not converge to real values. Even though, the identification adjusts them to have a better fitting of the output predictions with the output measures, what represent a refinement in the model. This makes the identification useful for a refinement of the controller gains, in any case.

Different combinations of output signals were examined, and efficient identification was achieved by using pitch angular velocity, angle of attack, altitude and speed, while the angle of pitch was considered irrelevant.

7. ACKNOWLEDGEMENTS

The second author thanks CNPq for the financial support.

8. REFERENCES

Briggs, M. M., 1992. “Systematic Tactical Missile Design”. In: *Tactical Missile Aerodynamics: General Topics*. p. 94. American Institute of Aeronautics and Astronautics. Hampton, Virginia.

Coelho, F. A. A., 2007. *Modelagem, Controle e Simulação Hardware in the Loop de um Míssil com Vôo Rasante à Superfície do Mar*. Master thesis, COPPE UFRJ, Rio de Janeiro.

Dorfling, J. & Rokhsaz, K., 2014. *Non-Linear Aerodynamic Modeling of Airfoils for Accurate Blade Element Propeller Performance Predictions*. Atlanta, GA, AIAA Aviation, pp. 1-16.

Hou, M.-Z. & Duan, G.-R., 2011. “Adaptive Dynamic Surface Control for Integrated Missile Guidance and Autopilot”. In *International Journal of Automation and Computing*, 8 February, pp. 122-127.

Jategaonkar, R. V., 2006. “Flight Vehicle System Identification: A Time Domain Methodology”. In *Progress in Astronautics Andaeronautics*. Vol. 216. American Institute of Aeronautics and Astronautics. Arlington, Texas.

Laminar Research, 2010. “Plane Maker Video Tutorials”. 26 Feb. 2015 <http://wiki.x-plane.com/Plane_Maker_Video_Tutorials>.

Laminar Research, 2015. “X-Plane 9 Desktop Manual”. 14 Apr. 2015 <http://wiki.x-plane.com/Appendix_A:_How_X-Plane_Works>.

Ribeiro, L. R., 2011. *Plataforma de Testes para Sistemas de Piloto Automático Utilizando Matlab/Simulink e Simulador de Voo X-Plane*. Master thesis, Instituto Tecnológico de Aeronáutica, São José dos Campos, Brazil.

Ridluan, A., 2014. “CFD investigation of compressible low angles of attack flow over the missile”. In *Journal of Physical Science and Application*, pp. 339-347.

Sooy, T. J. & Shmidt, R. Z., 2004. “Aerodynamic predictions, comparisons, and validations using Missile DATCOM (97) and Aeroprediction 98 (AP98)”. In *42nd AIAA Aerospace Sciences Meeting and Exhibit*. Reno, Nevada.

9. RESPONSIBILITY NOTICE

The authors are the only responsible for the printed material included in this paper.